Journal of Materials Chemistry C

PAPER

View Article Online
View Journal | View Issue

Cite this: J. Mater. Chem. C, 2015, 3, 12403

Investigation of the enhanced performance and lifetime of organic solar cells using solution-processed carbon dots as the electron transport layers†

Haijun Zhang,[a] Qian Zhang,[bc] Miaomiao Li,[bc] Bin Kan,[bc] Wang Ni,[bc] Yunchuang Wang,[bc] Xuan Yang,[bc] Chenxia Du,*[a] Xiangjian Wan[bc] and Yongsheng Chen*[bc]

Received 17th September 2015,
Accepted 12th November 2015

DOI: 10.1039/c5tc02957k

www.rsc.org/MaterialsC

Easily prepared and stable solution-processed carbon dots (CDs) have been used and systematically investigated as the electron transport layers (ETLs) for both small-molecule and polymer-based solar cells. Significantly enhanced device performance and lifetime are observed. The enhanced performance is mainly driven by the improvements of the short circuit current (J_{sc}) and the fill factor (FF), caused by decreasing the work function of Al electrodes and series resistance, increasing shunt resistances, and balancing electrons and hole mobility. Therefore, the devices with CDs as the ETLs have higher charge transport and collection efficiency. In addition, lifetimes of the devices with CDs as the ETLs are also significantly improved, due to the much better air-stability of CD materials compared to LiF as the ETLs. And another reason is that it can efficiently prevent the formation of an unstable cathode contact for the diffusion of Al ions at the interface. These results indicate that CDs, relatively cheap and stable materials, have great potential to be promising ETL materials for industrial-scale manufacture of organic solar cells.

Introduction

Organic photovoltaic cells (OPVs) have attracted enormous attention as promising alternatives to conventional fossil resources due to their unique advantages, including low cost, light weight, mechanical flexibility and solution processability.[1] Moreover, solution processability allows the low-cost fabrication of large-area by roll-to-roll (R2R) printing, in contrast to traditional Si-based solar cells. Recently, power conversion efficiencies (PCEs) of over 10% have been achieved for both polymers and small-molecule based solar cells with bulk-heterojunction (BHJ) architecture.[2–6] Organic solar cells have sandwich structures including photoactive layers, interfacial buffer layers, and electrodes. Up to now, the advancement of record-high PCEs has been mainly driven by the synthesis of novel electron-donor polymers[7–10] and small molecules,[11–14] and electron-acceptor materials,[15–17] along with device optimization processing.[11,12,18–20] Therefore, interfacial engineering also plays a critical role in determining the performance of OPVs.[21,22] Better interfacial layers contribute to providing better energy alignment, minimizing contact resistance and realizing ohmic contacts between the active layer and the electrodes for better charge extraction.[23] Furthermore, the optimized interfacial layers could also prevent the recombination of electrons and holes by improving of the charge transport and extraction pathways.[24] So far, LiF[25] and Ca[26] as the ETLs have been widely used in OPVs. However, the thickness and the evaporation rate of those ETLs are difficult to control, which can also cause significant cost to the fabrication of large areas. Besides, these ETL materials are very sensitive to moisture and oxygen, causing the inferior device stability and operating lifetime. Thus, for future possible industrial applications, solution-processed ETLs with low synthesis cost, and high device performances repeatability and stability are highly needed. Recently, various solution-processed ETLs, such as nanoscale transition metal oxides (*e.g.* ZnO),[27] fullerene derivatives[28,29] and polyelectrolytes (*e.g.* PEI, PFN)[22,30]

[a] The College of Chemistry, Molecular Engineering, Zhengzhou University, Zhengzhou, 450052, P. R. China. E-mail: dcx@zzu.edu.cn
[b] State Key Laboratory and Institute of Elemento-Organic Chemistry, Collaborative Innovation Center of Chemical Science and Engineering (Tianjin), Nankai University, Tianjin 300071, China
[c] Key Laboratory of Functional Polymer Materials and the Centre of Nanoscale Science and Technology, Institute of Polymer Chemistry, College of Chemistry, Nankai University, Tianjin, 300071, China. E-mail: xjwan@nankai.edu.cn, yschen99@nankai.edu.cn

† Electronic supplementary information (ESI) available: General characterization, UV-vis, FT-IR,PL, XPS, TEM and XRD spectra of the CDs, AFM, SCLC, UPS figures, *etc.* See DOI: 10.1039/c5tc02957k

have been studied and in some cases give exciting performances. However, these materials in most cases, including the nano ZnO, are difficult to prepare and/or very expensive. And some previous studies based on graphene quantum dots (GQDs) as hole extraction layers have been reported in polymer solar cells, and GQDs could improve the lifetime and improving the contact between the blended polymer layers and anodes.[31–33]

Herein, carbon dots (CDs), easily synthesized from low-cost commercial off-the-shelf materials by a facile and efficient one-step strategy, were studied as the ETLs for both small-molecule solar cells (SMSCs) and polymer solar cells (PSCs) with the blend of small molecule DR3TBDTT:[6,6]-phenyl-C_{71}-butyric acid methyl ester (DR3TBDTT:$PC_{71}M$) and poly(3-hexylthiophene):[6,6]-phenyl-C_{61}-butyric acid methyl ester (P3HT:$PC_{61}BM$) as the active layer, respectively. As a result, significantly improved both performance and lifetimes were observed. Furthermore, the cells with CDs as the ETLs exhibited excellent reproducibility using an environmentally friendly solvent (methanol).

Results and discussion

CDs synthesis and characterization

CDs were prepared following the literature[34] (see the Experimental section for the details) with slight modification, and characterized using various spectroscopic methods (see Fig. S1–S6, ESI†). Fig. S3 (ESI†) shows the fluorescence spectra of the CDs, which exhibit an excitation-dependent emission phenomenon. The TEM image shows that our CDs are of uniform sizes and have a narrow distribution in the range of 1–2 nm (Fig. S5, ESI†).

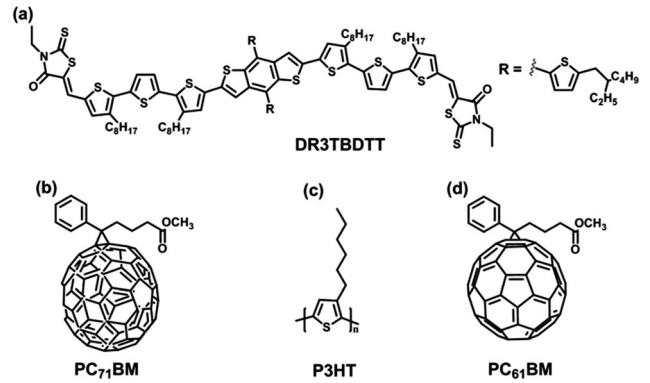

Scheme 1 Molecular structures of (a) DR3TBDTT, (b) $PC_{71}BM$, (c) P3HT, and (d) $PC_{61}BM$.

CDs as the ETLs for small molecule based device

The photovoltaic performances of small-molecule solar cells with CDs as the ETLs prepared from CD methanol solutions with different concentrations, together with the control devices, are systematically investigated. The thickness of CD based ETL can be easily controlled by using different concentrations of CDs solution and partially cover the active layer (see Fig. S7 and Table S1 for the details, ESI†). The cell structure is ITO/PEDOT:PSS/DR3TBDTT:$PC_{71}BM$/ETLs/Al. The molecular structures of DR3TBDTT and $PC_{71}BM$ are displayed in Scheme 1a and b, respectively. The average device performance parameters (based on min of 30 devices) with CDs of various concentrations and the control/compared devices without ETL/with LiF as the ETLs under the illumination of AM 1.5G, 100 mW cm^{-2} are summarized in Table 1. Typical current density *versus* voltage (*J*–*V*) curves of the devices are shown in Fig. 1a. The device without an ETL exhibits an average PCE of 7.00% with a V_{oc} of 0.895 V, a J_{sc} of 12.88 mA cm^{-2}, and an FF of 60.8%. The device with LiF as the ETL exhibits an average PCE of 7.22% with a V_{oc} of 0.91 V, a J_{sc} of 12.92 mA cm^{-2}, and an FF of 61.8%.[11] Notably, using solution-processed CDs with various concentrations as the ETLs, the devices clearly exhibit enhanced performance compared to that of the device without an ETL and more importantly that of the device with LiF as the ETL. The device with CDs at the optimal concentration (0.1 mg mL^{-1}) as the ETLs exhibits an average PCE of 7.67% with a V_{oc} of 0.904 V, a J_{sc} of 13.32 mA cm^{-2}, and an FF of 63.7%. From Table 1, the series resistance (R_s) decreases from 13.1 to 11.7 and 9.3 Ω cm^{-2}, and shunt resistances (R_{sh}) increases significantly from 716.9 to 1134.7 and 1577.1 Ω cm^{-2} for the device without an ETL, the device with LiF as the ETL, and the device with CDs (0.1 mg mL^{-1}) as the ETLs, respectively. Thus, the reduced R_s and increased R_{sh} are expected to improve the ohmic contact and reduce the leakage current (Fig. S8, ESI†), and therefore, higher FFs are observed for the device with CDs as the ETLs. In addition, the electron mobility measurements based on the space-charge limited current (SCLC) model with the device structure Al/DR3TBDTT:$PC_{71}BM$/ETLs/Al are shown in Fig. S9 (ESI†) and the results are also summarized in Table 1. The hole mobility[11] of 2.88 × 10^{-4} cm^2 V^{-1} s^{-1} was measured with the

Table 1 Average OPV performance parameters for DR3TBDTT : $PC_{71}BM$ (1 : 0.8 w/w) based solar cells with the various ETLs (device structure, ITO/PEDOT:PSS/DR3TBDTT:$PC_{71}BM$/ETL/Al), along with the shunt resistance (R_{sh}) and series resistance (R_s) and electron mobility

ETL	V_{oc} (V)	J_{sc} (mA cm^{-2})	FF (%)	PCE[a] (%)	R_s (Ω cm^{-2})	R_{sh} (Ω cm^{-2})	μ_e (cm^2 V^{-1} s^{-1})
None[b]	0.895	12.88	60.8	7.00(7.19)	13.1	716.9	4.39 × 10^{-4}
LiF[c]	0.910	12.92	61.8	7.22(7.51)	11.7	1134.7	3.44 × 10^{-4}
1.0 mg mL^{-1} [d]	0.903	13.02	61.3	7.20(7.33)	11.2	428.5	2.32 × 10^{-4}
0.5 mg mL^{-1} [d]	0.903	13.01	61.9	7.27(7.39)	9.4	1454.1	2.62 × 10^{-4}
0.1 mg mL^{-1} [d]	**0.904**	**13.32**	**63.7**	**7.67(7.78)**	**9.3**	**1577.1**	**3.06 × 10^{-4}**
0.05 mg mL^{-1} [d]	0.905	13.12	62.8	7.45(7.52)	11.5	1123.0	3.41 × 10^{-4}
0.01 mg mL^{-1} [d]	0.904	13.03	61.4	7.23(7.48)	12.1	1104.2	4.30 × 10^{-4}

[a] The best efficiency is shown in parentheses. [b] The devices without ETLs. [c] The devices with LiF as the ETLs, the data are from ref. 11. [d] The devices with CDs of various concentrations as the ETLs. All the data are based on the results of 15 devices.

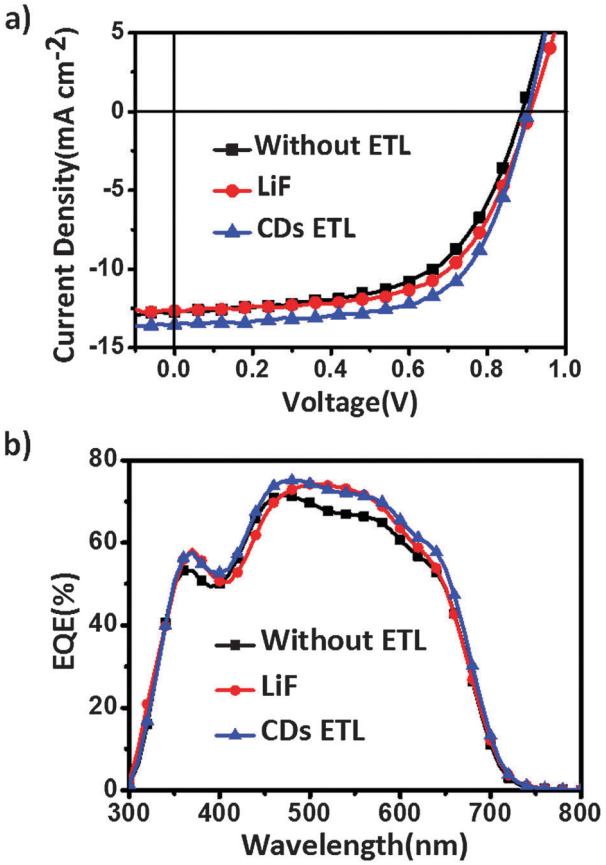

Fig. 1 (a) Current density *versus* voltage (*J*–*V*) curves and (b) external quantum efficiency (EQE) curves characteristics for the devices without ETLs (squares), with LiF as the ETL (circles), and with CDs of the optimal concentration as the ETLs (up-triangles, 0.1 mg mL^{-1}). All the devices under simulated 100 mW cm^{-2} AM 1.5G illumination.

device structure ITO/PEDOT:PSS/DR3TBDTT:$PC_{71}BM$/MoO_3/Au. The electron mobility for the device with CDs (0.1 mg mL^{-1}) was measured with a value of 3.06×10^{-4} cm^2 V^{-1} s^{-1}. Thus, more balanced charge transport in the device is achieved. This may increase the FF by restricting the build-up of space charges, and hence, reducing charge recombination.

The external quantum efficiency (EQE) spectra of the DR3TBDTT based devices with CDs as the ETLs and the compared devices are investigated as shown in Fig. 1b. The EQE curve for the device with CDs (0.1 mg mL^{-1}) as the ETLs exhibits better response than those of devices without ETLs, and with LiF as the ETL. Especially, the EQE curve for the device with CDs (0.1 mg mL^{-1}) exceeds 70% in a wide range of 450–600 nm with the maximum value of over 75% at 490 nm. In comparison, the device without an ETL, and the device with LiF as the ETL show peaks of 71% at 470 nm, and 74% at 510 nm, respectively. All the calculated J_{sc} values obtained by the integration of the EQE data agree well with the J_{sc} values from the *J*–*V* measurements. These results prove that CDs as the ETLs could indeed improve the J_{sc}.

The increased J_{sc} in the OPV devices may originate from reduced bimolecular recombination, the increased absorption of photons, or a combination of both.[35] To gain deeper insight into the influence of the CD buffer layers on the device performances, photocurrent density *versus* effective voltage (J_{ph}–V_{eff}) characteristics are investigated for the devices with or without ETLs under constant incident light intensity (AM 1.5G, 100 mW cm^{-2}). $J_{ph} = J_L - J_D$, where J_L and J_D are the current densities under illumination and in the dark, respectively. For $V_{eff} = V_0 - V_{appl}$, V_0 is the voltage at $J_{ph} = 0$ and V_{appl} is the applied voltage.[12,22] A plot of J_{ph} *versus* V_{eff} in a wide reverse-bias range is presented in Fig. 2a. Notably, J_{ph} reaches saturation for these devices at a large reverse voltage (*e.g.* V_{eff} = 2.5 V, see Fig. S10 (ESI†) for the detailed J_{ph}–V_{eff} without the log graph), which suggests that at this voltage the photogenerated excitons are dissociated into free carriers and the carriers are collected by the electrodes with little geminate or bimolecular recombination. The ratio J_{ph}/J_{sat} can be used to judge the overall exciton dissociation efficiency and charge collection efficiency.[36] Under short-circuit conditions, the ratios $J_{ph,sc}/J_{ph,sat}$ are 92.4%, 93.4%, and 96.1% for the device without an ETL, the device with LiF as the ETL, and the device with CDs (0.1 mg mL^{-1}) as the ETLs, respectively. Under the maximal power output conditions, for the device without an ETL, the device with LiF as the ETL, and the device with CDs (0.1 mg mL^{-1}) as the ETLs, $J_{ph,m}/J_{ph,sat}$ are 78.3%, 77.5%, and 81.3%, respectively. These results indicate that the device with CDs (0.1 mg mL^{-1})

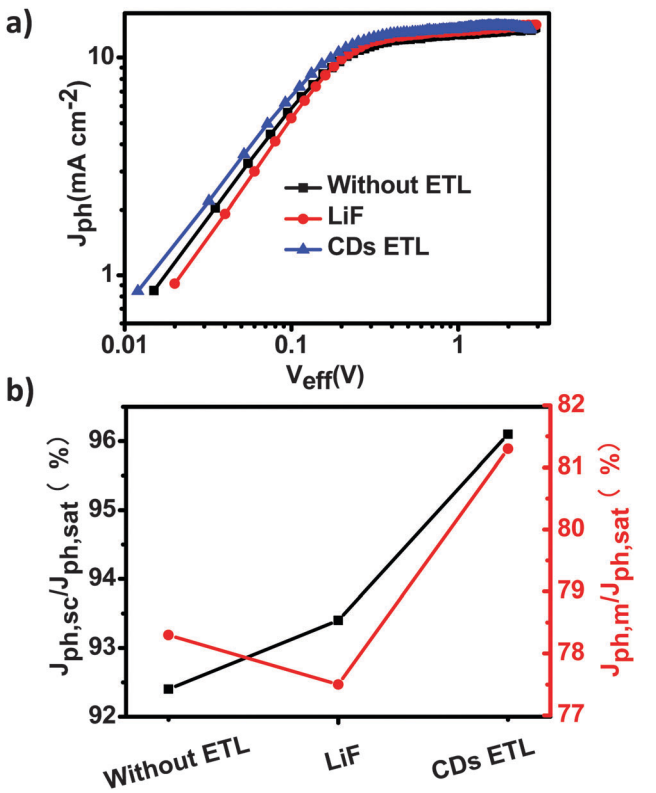

Fig. 2 (a) Photocurrent density *versus* effective voltage (J_{ph}–V_{eff}) and (b) correlation $J_{ph,sc}/J_{ph,sat}$ and $J_{ph,m}/J_{ph,sat}$ characteristics for the devices without ETLs (squares), with LiF as the ETL (circles), and with CDs of the optimal concentration as the ETLs (up-triangles, 0.1 mg mL^{-1}). All the devices under constant incident light intensity simulated 100 mW cm^{-2} AM 1.5G illumination.

as the ETL has higher exciton dissociation and charge collection efficiency (Fig. 2b). Though the overall performance is limited by using CDs as the ETLs compared with that when using LiF as the ETL, the superior J_{ph}–V_{eff} characteristics of devices clearly demonstrate that CDs as the ETLs can reduce bimolecular recombination and increase charge collection efficiency. In addition, a lower work function (−3.56 *vs.* −4.3 eV, Fig. S11 and Table S2, ESI†)[37] is also observed for the Al electrode when CDs are used as the ETLs. This should generate a higher built-in voltage (V_{bi}), which is believed to facilitate the change extraction/separation. Thus, higher J_{sc} value of the device with CDs as the ETLs is observed. And the absorption spectra of the blends and CDs (0.1 mg mL^{-1}) spin-coated onto the active layer are showed in Fig S12 (ESI†). There was nearly no difference in the absorption. So reduced bimolecular recombination might be the dominant factor.

Enhanced lifetime using CDs as the ETLs

One of the most challenging issues for OPVs is their limited lifetime. To investigate the stability and feasibility for large-scale organic solar cells manufacture, lifetime testing experiments of SMSCs with different ETLs are conducted. The stability testing used in this analysis was in accordance with ISOS-D-1 protocols.[38] All the devices are simply sealed by ultraviolet-curable resins and without other complicated encapsulation techniques, and are stored in a glove box or in air (humidity, 60%; 25 °C). Fig. 3 shows PCEs degradation over time for the device without an ETL, the device with LiF as the ETL, and the device with CDs (0.1 mg mL^{-1}) as the ETLs. As shown in Fig. 3, the degradation of photovoltaic performance for the device with CDs (0.1 mg mL^{-1}) is much slower than that of the devices without ETLs, and with LiF as the ETL in both the glove box and air. The PCE of the device with LiF as the ETL drops rapidly to 54% of an initial PCE in air after 1970 min (~33 h) and 53% of an initial PCE in the glove box for 10 220 min (170 h). In contrast, the device with CDs (0.1 mg mL^{-1}) remains the PCE near 90% of the initial PCE under the same conditions in the glove box. And even in air, the device with CDs (0.1 mg mL^{-1}) also has the PCE over 85% of the initial PCE after 11 150 min (~186 h) (see Fig. S13–S16 for the detailed degradation data in the ESI†). This should be due to the much better air-stability of CD materials to both moisture and oxygen, compared to LiF as the ETLs. Another reason may be that CDs as the ETLs can efficiently prevent the diffusion of Al ions during the evaporation process. Metal ions formed at the interface tend to migrate into the active layer and form an unstable cathode contact, thus further affect the performance and long-term stability of the devices.[37,39] These results indicate that the devices with CDs (0.1 mg mL^{-1}) as the ETLs have a much improved operational stability.

In addition, Table S3 (ESI†) exhibits a statistical analysis of 15 high performance devices for each ETL, showing the reproducible differences for V_{oc}, J_{sc}, FF and PCE. The photovoltaic parameters of CDs (0.1 mg mL^{-1}) as the ETLs show overall significantly lower standard deviations (σ), confirming that the cells exhibit better reproducibility for cell performance.

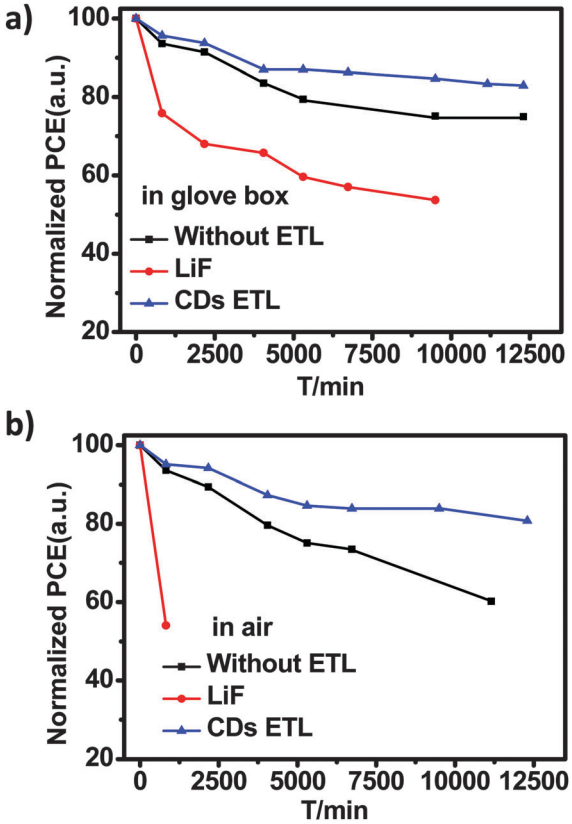

Fig. 3 The normalized efficiency *vs.* storage time for the conventional devices without ETLs (squares), with LiF as the ETL (circles), and with CDs of the optimal concentration as the ETLs (up-triangles, 0.1 mg mL^{-1}) stored (a) in a glove box and (b) in air (humidity, 60%; 25 °C) with simple encapsulation.

CDs as the ETLs for polymer-based devices

To further test the applicability of CDs in OPV cells, we investigated the CDs as the ETLs in polymer solar cells using the landmark material poly(3-hexylthiophene):phenyl-C_{61}-butyric acid methyl ester (P3HT:$PC_{61}BM$) as the donor. The average device performance parameters with CDs of the various concentrations and the control devices without ETLs under the illumination of AM 1.5G, 100 mW cm^{-2} are summarized in Table 2. The typical *J*–*V* curves of the optimized devices shown in Fig. S17 (ESI†) indicate that the CDs as the ETLs has the similar performance as that for the small molecule based devices studied above. For example, the device without an ETL exhibits an average PCE of 3.06% (best PCE 3.08%) with a V_{oc} of 0.610 V, an FF of 50.4%, and a J_{sc} of 9.98 mA cm^{-2}. The device with LiF as the ETL exhibits an average PCE of 3.38% with a V_{oc} of 0.604 V, a J_{sc} of 10.03 mA cm^{-2}, and an FF of 55.8%. Notably, the devices with CDs (0.5 mg mL^{-1}) give an average PCE of 3.42% (best PCE 3.52%) with a V_{oc} of 0.609 V, an FF of 54.8%, and a J_{sc} of 9.98 mA cm^{-2}. These results indicate the wide applicability of CDs as the ETL materials.

Conclusions

In conclusion, easily made solution-processed CDs have been synthesized and investigated as the ETLs for both small-molecule

Table 2 Average OPV performance parameters for bulk heterojunction (BHJ) solar cells based on P3HT : $PC_{61}BM$ (1 : 1 w/w) with or without ETLs, along with the shunt resistance (R_{sh}) and series resistance (R_s)

ETL	V_{oc} (V)	J_{sc} (mA cm^{-2})	FF (%)	PCE[a] (%)	R_s (Ω cm^{-2})	R_{sh} (Ω cm^{-2})
None[b]	0.610	9.98	50.4	3.06(3.08)	14.6	373.0
LiF[c]	0.604	10.03	55.8	3.38(3.46)	13.2	643.2
1.0 mg mL^{-1} [d]	0.609	10.11	51.7	3.18(3.29)	13.5	623.8
0.5 mg mL^{-1} [d]	**0.609**	**10.25**	**54.8**	**3.42(3.52)**	**12.3**	**691.6**
0.1 mg mL^{-1} [d]	0.608	10.13	52.8	3.25(3.34)	11.7	694.1
0.05 mg mL^{-1} [d]	0.613	9.86	0.521	3.15(3.21)	13.4	631.2

[a] The best efficiency is shown in parentheses. [b] The devices without ETLs. [c] The reference devices with LiF as the ETLs. [d] The devices with CDs of various concentrations as the ETLs. All the data are based on the results of 15 devices.

and polymer based solar cell devices and much improved performances have achieved in terms of both power conversion efficiency and life stability. The enhanced PCEs are due to the improvement of J_{sc} and FF, mainly due to the reduced series resistance, increased shunt resistance, together with the lower work function of the electrode. In addition, the device lifetime is also improved significantly, due to by the much better air-stability of CD materials compared to LiF as the ETLs. Another reason may be that CDs as the ETLs can efficiently prevent the formation of an unstable cathode contact for the diffusion of Al ions at the interface into the active layer. Compared with the currently widely used ETL materials such as LiF and Ca, these results demonstrate that the easily prepared, cheap and stable carbon dots could be used as efficient ETL materials for both small-molecule and polymer based OPV devices, which might hold some significance for future commercialization of OPV devices.

Experimental section

Materials preparation

DR3TBDTT was synthesized using the method reported previously.[11] P3HT was purchased from Rieke Metals, Inc. $PC_{71}BM$ and $PC_{61}BM$ were purchased from American Dye Source, Inc. All of the materials are used as received unless otherwise specified.

Preparation of carbon dots

Carbon dots were prepared following the literature with slight modification.[34] In a typical synthesis, citric acid (2.1014 g) and ethylenediamine (670 μL) were dissolved in DI-water (30 mL). Then the solution was transferred into a poly (tetrafluoroethylene) (Teflon)-lined autoclave (50 mL) and heated to 250 °C for 10 h. After cooling to room temperature, the reaction solution was filtered through a 0.22 μm microporous membrane and a brown-black filter solution was obtained, which was further dialyzed in a dialysis bag (retained molecular weight: 1000 Da) for 5 days and the CDs were obtained by vacuum freeze-drying.

Device fabrication

Devices are fabricated with a structure of glass/ITO/PEDOT:PSS/donor:acceptor/ETL/Al. The ITO-coated glass substrates are cleaned by an ultrasonic treatment in detergent, deionized water, acetone and, isopropyl alcohol under ultrasonication for 15 min each, and subsequently dry by a nitrogen blow. A thin layer of PEDOT:PSS (Clevios P VP AI 4083, filtered at 0.45 μm) is spin-coated at 4500 rmp onto the ITO surface. After being baked at 150 °C for 20 min, the substrates are transferred into an argon-filled glove box. Subsequently, the active layer is spin-coated on the HTLs. For the small-molecule solar cells, the chloroform solution containing 10 mg mL^{-1} of DR3TBDTT and 8.0 mg mL^{-1} of $PC_{71}BM$ is spin-cast onto the HTLs at 1700 rpm for 20 s. For the polymer solar cells, the *o*-dichlorobenzene (*o*-DCB) solution containing 18 mg mL^{-1} of P3HT and 18 mg mL^{-1} of $PC_{61}BM$ is spin-coated at 800 rpm for 18 s. The resulting active-coated substrates are kept in a petri dish at room temperature for 1 h to allow the *o*-DCB solvent to evaporate slowly, and then they are annealed inside the glove box at 110 °C for 10 min. Finally, the various concentrations of CDs using a methanol solution as ETLs are spin-coated onto the active layer and then the 80 nm Al layer is evaporated under high vacuum ($< 2 \times 10^{-4}$ Pa). The effective areas of cells are 4 mm^2, defined by shadow masks.

Characterization

UV-vis absorption spectra are obtained using a JASCO V-570 spectrometer. Fourier transform infrared (FT-IR) spectra are recorded on a Bruker Tensor 27 spectrometer (Germany). Photoluminescence characterization is carried out using a FluoroMax-P luminescence spectrometer using a xenon lamp as the source of excitation. X-ray photoelectron spectroscopy (XPS) analysis is performed using an AXIS HIS 165 spectrometer (Kratos Analytical) with a monochromatized Al Kα X-ray source (1486.71 eV photons). An X-ray diffraction (XRD) experiment is performed on a Bruker D8 FOCUS X-ray diffractometer with Cu Kα radiation (k = 1.5406 Å) at a generator voltage of 40 kV and a current of 40 mA. Transmission electron microscopy (TEM) is performed on a Philips Technical G^2 F20 at 200 kV. Atomic force microscopy (AFM) investigation is carried out using a Bruker Multi Mode 8 instrument in the "tapping" mode. The ultraviolet photoelectron spectroscopy (UPS) measurements (Thermo ESCALAB 250) are carried out using the He I ($h\nu$ = 21.2 eV) source.

The *J*–*V* curves for the photovoltaic devices are obtained using a Keithley 2400 source-measure unit. The photocurrent is measured under simulated 100 mW cm^{-2} AM 1.5G irradiation using an Oriel 96000 solar simulator calibrated with a standard Si solar cell. The average PCE is obtained using 15 high performance devices under the same conditions.

The EQE values of the encapsulated devices are measured using a lock-in amplifier (SR810, Stanford Research Systems).

The devices are illuminated by monochromatic light from a 150 W xenon lamp passing through an optical chopper and a monochromator. The photon flux is determined by a calibrated standard silicon photodiode.

Mobility measurements are performed with the following diode structures: Al/DR3TBDTT:$PC_{71}BM$/ETL/Al for the electron at the *J–V* curve in the range of 0–7 V. The charge carrier mobility is calculated using the space-charge limited current (SCLC)[40] model:

$$J = \frac{9\varepsilon_0\varepsilon_r\mu_0 V^2}{8L^3}\exp\left(0.89\beta\sqrt{\frac{V}{L}}\right)$$

in which J is the current density, L is the film thickness of the active layer, μ_0 is the zero-field electron mobility, ε_r is the relative dielectric constant of the transport medium, ε_0 is the permittivity of free space (8.85×10^{-12} F m^{-1}), β is the field activation factor, and V ($=V_{appl} - V_{bi}$) is the internal voltage in the device, in which V_{appl} is the applied voltage to the device and V_{bi} is the built-in voltage caused by the relative work function difference of the two electrodes.

Detailed encapsulation techniques procedure: we took a bit UV-curable EPOXY resin on the device; and then put a cover glass on the glue; finally UV-curable process was followed when the glue covered the devices.

Acknowledgements

The authors gratefully acknowledge for financial support from MoST (2014CB643502), NSFC (51373078, 51422304, 91433101, 21371154), PCSIRT (IRT1257), Tianjin city (13RCGFGX01121).

References

1 J. Kesters, T. Ghoos, H. Penxten, J. Drijkoningen, T. Vangerven, D. M. Lyons, B. Verreet, T. Aernouts, L. Lutsen, D. Vanderzande, J. Manca and W. Maes, *Adv. Energy Mater.*, 2013, **3**, 1180.
2 S.-H. Liao, H.-J. Jhuo, P.-N. Yeh, Y.-S. Cheng, Y.-L. Li, Y.-H. Lee, S. Sharma and S.-A. Chen, *Sci. Rep.*, 2014, **4**, 6813.
3 J.-D. Chen, C. Cui, Y.-Q. Li, L. Zhou, Q.-D. Ou, C. Li, Y. Li and J.-X. Tang, *Adv. Mater.*, 2015, **27**, 1035.
4 B. Kan, M. Li, Q. Zhang, F. Liu, X. Wan, Y. Wang, W. Ni, G. Long, X. Yang, H. Feng, Y. Zuo, M. Zhang, F. Huang, Y. Cao, T. P. Russell and Y. Chen, *J. Am. Chem. Soc.*, 2015, 137.
5 H. Kang, S. Kee, K. Yu, J. Lee, G. Kim, J. Kim, J.-R. Kim, J. Kong and K. Lee, *Adv. Mater.*, 2015, **27**, 1408.
6 C. Liu, C. Yi, K. Wang, Y. Yang, R. S. Bhatta, M. Tsige, S. Xiao and X. Gong, *ACS Appl. Mater. Interfaces*, 2015, **7**, 4928.
7 Y. Li, *Acc. Chem. Res.*, 2012, **45**, 723.
8 H. Zhou, L. Yang and W. You, *Macromolecules*, 2012, **45**, 607.
9 J. E. Coughlin, Z. B. Henson, G. C. Welch and G. C. Bazan, *Acc. Chem. Res.*, 2014, **47**, 257.
10 L. Lu and L. Yu, *Adv. Mater.*, 2014, **26**, 4413.
11 J. Zhou, Y. Zuo, X. Wan, G. Long, Q. Zhang, W. Ni, Y. Liu, Z. Li, G. He, C. Li, B. Kan, M. Li and Y. Chen, *J. Am. Chem. Soc.*, 2013, **135**, 8484.
12 Q. Zhang, B. Kan, F. Liu, G. Long, X. Wan, X. Chen, Y. Zuo, W. Ni, H. Zhang, M. Li, Z. Hu, F. Huang, Y. Cao, Z. Liang, M. Zhang, T. P. Russell and Y. Chen, *Nat. Photonics*, 2014, **9**, 35.
13 Y. Chen, X. Wan and G. Long, *Acc. Chem. Res.*, 2013, **46**, 2645.
14 M. Moon, B. Walker, J. Lee, S. Y. Park, H. Ahn, T. Kim, T. H. Lee, J. Heo, J. H. Seo, T. J. Shin, J. Y. Kim and C. Yang, *Adv. Energy Mater.*, 2015, **5**, 1402044.
15 Y. He, H.-Y. Chen, J. Hou and Y. Li, *J. Am. Chem. Soc.*, 2010, **132**, 1377.
16 Y. Liu, C. Mu, K. Jiang, J. Zhao, Y. Li, L. Zhang, Z. Li, J. Y. L. Lai, H. Hu, T. Ma, R. Hu, D. Yu, X. Huang, B. Z. Tang and H. Yan, *Adv. Mater.*, 2015, **27**, 1015.
17 X. Zhang, Z. Lu, L. Ye, C. Zhan, J. Hou, S. Zhang, B. Jiang, Y. Zhao, J. Huang, S. Zhang, Y. Liu, Q. Shi, Y. Liu and J. Yao, *Adv. Mater.*, 2013, **25**, 5791.
18 A. K. K. Kyaw, D. H. Wang, D. Wynands, J. Zhang, T.-Q. Nguyen, G. C. Bazan and A. J. Heeger, *Nano Lett.*, 2013, **13**, 3796.
19 S.-H. Liao, H.-J. Jhuo, P.-N. Yeh, Y.-S. Cheng, Y.-L. Li, Y.-H. Lee, S. Sharma and S.-A. Chen, *Sci. Rep.*, 2014, **4**, 6813.
20 S. Zhang, L. Ye, W. Zhao, B. Yang, Q. Wang and J. Hou, *Sci. China: Chem.*, 2015, **58**, 248–256.
21 K. Zhang, Z. Hu, R. Xu, X. F. Jiang, H. L. Yip, F. Huang and Y. Cao, *Adv. Mater.*, 2015, **27**, 3607.
22 G. Long, X. Wan, B. Kan, Z. Hu, X. Yang, Y. Zhang, M. Zhang, H. Wu, F. Huang, S. Su, Y. Cao and Y. Chen, *ChemSusChem*, 2014, **7**, 2358.
23 J. Zhu, F. Bebensee, W. Hieringer, W. Zhao, J. H. Baricuatro, J. A. Farmer, Y. Bai, H.-P. Steinrück, J. M. Gottfried and C. T. Campbell, *J. Am. Chem. Soc.*, 2009, **131**, 13498.
24 M. J. Beliatis, K. K. Gandhi, L. J. Rozanski, R. Rhodes, L. McCafferty, M. R. Alenezi, A. S. Alshammari, C. A. Mills, K. D. G. I. Jayawardena, S. J. Henley and S. R. P. Silva, *Adv. Mater.*, 2014, **26**, 2078.
25 C. J. Brabec, S. E. Shaheen, C. Winder, N. S. Sariciftci and P. Denk, *Appl. Phys. Lett.*, 2002, **80**, 1288.
26 M. O. Reese, M. S. White, G. Rumbles, D. S. Ginley and S. E. Shaheen, *Appl. Phys. Lett.*, 2008, **92**, 053307.
27 Y. Sun, J. H. Seo, C. J. Takacs, J. Seifter and A. J. Heeger, *Adv. Mater.*, 2011, **23**, 1679.
28 C.-H. Hsieh, Y.-J. Cheng, P.-J. Li, C.-H. Chen, M. Dubosc, R.-M. Liang and C.-S. Hsu, *J. Am. Chem. Soc.*, 2010, **132**, 4887.
29 K. M. O'Malley, C.-Z. Li, H.-L. Yip and A. K. Y. Jen, *Adv. Energy Mater.*, 2012, **2**, 82.
30 H. Kang, S. Hong, J. Lee and K. Lee, *Adv. Mater.*, 2012, **24**, 3005.
31 C. X. Guo, H. B. Yang, Z. M. Sheng, Z. S. Lu, Q. L. Song and C. M. Li, *Angew. Chem., Int. Ed.*, 2010, **49**, 3014–3017.
32 H. Bin Yang, Y. Qian Dong, X. Wang, S. Yun Khoo, B. Liu and C. Ming Li, *Sol. Energy Mater. Sol. Cells*, 2013, **117**, 214–218.
33 Z. Ding, Z. Hao, B. Meng, Z. Xie, J. Liu and L. Dai, *Nano Energy*, 2015, **15**, 186–192.

34 S. Zhu, Q. Meng, L. Wang, J. Zhang, Y. Song, H. Jin, K. Zhang, H. Sun, H. Wang and B. Yang, *Angew. Chem., Int. Ed.*, 2013, **52**, 3953.
35 Z. He, C. Zhong, S. Su, M. Xu, H. Wu and Y. Cao, *Nat. Photonics*, 2012, **6**, 591.
36 Z. He, C. Zhong, X. Huang, W. Y. Wong, H. Wu, L. Chen, S. Su and Y. Cao, *Adv. Mater.*, 2011, **23**, 4636.
37 J. Min, Y. N. Luponosov, Z.-G. Zhang, S. A. Ponomarenko, T. Ameri, Y. Li and C. J. Brabec, *Adv. Energy Mater.*, 2014, **4**, 1400816.
38 M. O. Reese, S. A. Gevorgyan, M. Jørgensen, E. Bundgaard, S. R. Kurtz, D. S. Ginley, D. C. Olson, M. T. Lloyd, P. Morvillo, E. A. Katz, A. Elschner, O. Haillant, T. R. Currier, V. Shrotriya, M. Hermenau, M. Riede, K. R. Kirov, G. Trimmel, T. Rath, O. Inganäs, F. Zhang, M. Andersson, K. Tvingstedt, M. Lira-Cantu, D. Laird, C. McGuiness, S. Gowrisanker, M. Pannone, M. Xiao, J. Hauch, R. Steim, D. M. DeLongchamp, R. Rösch, H. Hoppe, N. Espinosa, A. Urbina, G. Yaman-Uzunoglu, J.-B. Bonekamp, A. J. J. M. van Breemen, C. Girotto, E. Voroshazi and F. C. Krebs, *Sol. Energy Mater. Sol. Cells*, 2011, **95**, 1253–1267.
39 I. Parker, Y. Cao and C. Yang, *J. Appl. Phys.*, 1999, **85**, 2441.
40 G. Malliaras, J. Salem, P. Brock and C. Scott, *Phys. Rev. B: Condens. Matter Mater. Phys.*, 1998, **58**, R13411.